

The overgrowth of structure-function coupling in premature brain during infancy

Rong Wang ^{a,b,c,d*}, Tianyu Fang ^{a,b,c,d}, Yue Zhang ^{a,b,c,d}, Yue Cheng ^e,
 Chunfang Wang ^f, Yuanyuan Chen ^{a,b,c,d,*}, Qiuyun Fan ^{a,b,c,d},
 Xin Zhao ^{a,b,c,d,*}, Dong Ming ^{a,b,c,d}

^a Medical School, Faculty of Medicine, Tianjin University, Tianjin, China

^b State Key Laboratory of Advanced Medical Materials and Devices, Tianjin University, Tianjin, China

^c Haihe Laboratory of Brain-Computer Interaction and Human-Machine Integration, Tianjin, China

^d Tianjin Key Laboratory of Brain Science and Neuroengineering, Tianjin, China

^e Department of Radiology, Tianjin First Central Hospital, Tianjin 300192, China

^f Tianjin Rehabilitation Institute, Tianjin 300121, China

ARTICLE INFO

Keywords:

Brain development
 Structure-function coupling
 Infant
 Functional MRI
 DTI

ABSTRACT

Although the rapid growth of brain structure and function during infancy has been well documented, relatively little is known about how these two developmental processes couple—an aspect that exhibits distinct patterns in adult brain. In this study, the multimodal MRI data from the dHCP database were used to investigate the coupling between brain structure and function in infants, with a particular focus on how prematurity influences this relationship. A similar pattern of the coupling distribution between preterm and full-term infants was identified with coupling index varying across unimodal cortices such as visual and sensorimotor regions and transmodal cortices including default mode network. Notably, a widespread overgrowth of structure-function coupling and a slow developmental trajectory towards full-term infants in preterm infants at term-equivalent age were found. Collectively, the study quantified the development of structure-function relationships in preterm infants, offering new insights into the information transmission processes and developmental patterns of the early-life brain.

1. Introduction

Infants traverse a period of remarkably swift and intricate brain development characterized by dynamic neural changes (Ouyang et al., 2019). During this intricate journey, the brains of preterm infants exhibit heightened sensitivity to environmental influences. The accelerated pace of brain maturation in preterm infants (Sun et al., 2023), coupled with the vulnerability to external factors (Boardman and Counsell, 2020), underscores the intricate interplay between genetic predispositions and environmental cues, subjecting them to risks of high mortality and neurocognitive impairments (Saigal and Doyle, 2008; Roze et al., 2021; Rees et al., 2022). Numerous research endeavors strive to identify the high-risks in preterm infants through the developmental trajectories of brain structure or function, thereby facilitating early intervention strategies. However, there are limited investigations exploring the developmental trajectory of preterm brain from the perspective of coupling brain structure and function, despite evidence

that these are highly coupled in the adult brain (Honey et al., 2009; Esfahlani et al., 2022).

Structural connectivity derived from diffusion-weighted imaging and functional connectivity obtained using fMRI signals respectively reflect the topological information and functional activities of the brain. Recent research on these two modalities in early brain development has advanced significantly, suggesting a synchrony in the development of brain structure and function. Both structural and functional connectivity develop in an orderly and region-specific pattern, with motor and sensory cortices maturing before the higher-order association cortices (Brenner et al., 2021; Eyre et al., 2021). Atypical structural and functional developments have been observed in infants with high genetic risks for brain disorders. For instance, infants at high genetic risks for autism spectrum disorders were found to have aberrant thalamocortical connectivity at both the functional and structural levels (Nair et al., 2021). Additionally, global structural network properties such as lower efficiency, longer connection distance, and fewer hub nodes and edges

* Correspondence to: No.92, Weijin Road, Nankai District, Tianjin 300072, China.

E-mail addresses: bain@tju.edu.cn (Y. Chen), zhaoxin@tju.edu.cn (X. Zhao).

were found in infants with a family history of schizophrenia compared to those without a family history of brain disorders (Shi et al., 2012). Furthermore, recent research on brain fingerprinting during infancy has found that structural connections are stable at birth (Girault et al., 2019; Ciarrusta et al., 2022), while functional connections mature progressively with age, and the accuracy of individual identification increases before the age of 2 (Hu et al., 2022). These findings indicate a certain level of consistency in structural and functional connectivity during infancy, potentially leading to similar coupling as seen in adults. However, existing studies have primarily focused on a single perspective (structural or functional), and research on the integrated structure-function relationship of the neonatal brain is extremely scarce. Since the brain's structure constrains and supports its functional activity (Honey et al., 2009; Sun et al., 2023), it is important to use multimodal analysis to study the complex relationship between brain structure and function in the perinatal period. Research has confirmed that the joint involvement of structure and function can identify preterm brains (Zhang et al., 2021), but there is a lack of a quantitative measure to assess the specific structure-function relationship.

Structure-function coupling has been identified as a potential biomarker for describing structural support for functional communication (Kulik et al., 2022) and has achieved significant success in adolescent and adult neuroscience research, providing crucial insights into understanding neurodisorders and brain development. Specifically, studies in mature brains have consistently demonstrated that structure-function coupling progressively decreases along cognitive representation hierarchies, with higher coupling in unimodal sensory regions such as visual, somatomotor and subcortical regions, and lower coupling in transmodal regions such as heteromodal association cortices, paralimbic regions, and limbic regions (Suárez et al., 2020; Gu et al., 2021; Fotiadis et al., 2023). Abnormal structure-function coupling has been frequently reported in populations with cognitive impairments, such as higher whole-brain coupling in patients with schizophrenia (van den Heuvel et al., 2013a; Collin et al., 2017), increased coupling within the default mode network (DMN) regions in patients with Alzheimer's disease (Dai et al., 2019), and the widespread decoupling across the brain in Parkinson's disease (Zarkali et al., 2021). In developmental brain studies, spatial distribution patterns of structure-function coupling similar to those in adults have been observed. From ages 8–23, coupling in higher cognitive regions shows a linear increase, while in visual regions, there is a slight decline (Baum et al., 2020). Another study with more detailed age intervals found that coupling in higher cognitive regions steadily increases from ages 9–14, while in visual regions, it rises initially before reaching a plateau (Soman et al., 2023). Furthermore, structure-function coupling has been proven to be a highly accurate identifier for brain states and individuals (Griffa et al., 2022), and it is highly stable within individuals over time (Gu et al., 2021). Collectively, these efforts highlight the tremendous potential of structure-function coupling as a biomarker.

Recent advancements in neonatal brain research have significantly enhanced our understanding of the structural and functional characteristics of the early brains. The population of premature infants is particularly noteworthy, as a substantial body of literature has documented the structural and functional differences between preterm and full-term brains (Rogers et al., 2018; Brenner et al., 2021). Research indicates that preterm infants exhibit weaker static functional connectivity strength (Damaraju et al., 2010; Thomason et al., 2017) and atypical patterns of dynamic functional connectivity (França et al., 2024) compared to their full-term infants. Additionally, the nodal properties of the structural network are significantly altered due to preterm birth (Zheng et al., 2023). However, the interplay between early brain structure and function remains inadequately understood. Given the pronounced differences in brain structure and function between preterm and full-term infants, it is imperative to investigate the relationship between these two domains. Consequently, we employed the structure-function coupling methodology, commonly utilized in adult

studies, to quantify this relationship and posited the hypothesis: (1) the coupling patterns in preterm brains are distinct, and (2) early coupling is associated with later behavioral outcomes. Extensive research in adults has demonstrated that abnormalities in structure-function coupling are associated with various neurocognitive impairments. Single-modal data from early brains have also shown correlations with behavioral outcomes at 18 months (Sun et al., 2023; França et al., 2024). To evaluate these hypotheses, we first examined the distribution of structure-function coupling in preterm and full-term infants. Subsequently, data were analyzed to illustrate the longitudinal growth of the coupling in preterm infants and its developmental trajectories for both groups. Finally, the relationship between early structure-function coupling and later cognitive, language, and motor performance was discussed. In summary, this study compared the developmental feature of structure-function coupling between preterm and full-term infants and revealed the overgrowth of the coupling in preterm infants.

2. Methods

2.1. Participants

All data were sourced from the third release of Developing Human Connectome Project (dHCP, <https://www.developingconnectome.org/>, Edwards et al., 2022), a substantial open science investigation into infant brain development. The study received ethical approval from the UK National Research Ethics Authority, and all participating families provided written consent before undergoing imaging sessions. This study included 436 full-term infants (202 females; mean gestational age at birth: 39.9 ± 1.27 weeks; mean PMA at scan: 41.14 ± 1.71 weeks) and 174 preterm infants (78 females, mean gestational age at birth: 32.24 ± 3.44 weeks), out of which 63 preterm infants provided longitudinal data and underwent two scans (PMA of 1st scan at birth: 34.49 ± 1.77 weeks; PMA at 2nd scan at term-equivalent age: 40.96 ± 2.10 weeks). Infants in both the preterm and full-term groups showed no evidence of major brain injury. Preterm infants were subdivided into Preterm at birth and at TEA (term-equivalent age) groups based on PMA (post menstrual age) at scan to assess differences between the two scans. To more accurately and scientifically assess the development of preterm infants, Preterm at TEA group, rather than Preterm at birth group, was considered for comparison with full-term infants. This was done to avoid exaggerated comparisons that may overlook compensatory growth in preterm infants during the period from birth to term-equivalent age. Behavioral outcomes were provided by dHCP, measured by Bayley Scales of Infant and Toddler Development, third edition (BSID-III), including cognition, language and motor performances assessed at age 20 months. Table 1 illustrates detailed information.

Table 1
Sample characteristics of full analysis sample.

Groups	Preterm		Full-term
	At birth	At TEA*	
Sex, num of females (%)	53/120 (44.17 %)	50/117 (42.74 %)	202/436 (46.33 %)
GA* at birth (weeks)	32.68 (2.45)	31.74 (3.78)	39.90 (1.27)
PMA* at scan (weeks)	34.49 (1.77)	40.96 (2.10)	41.14 (1.71)
Birth weight (kg)	1.63 (0.63)	1.73 (0.76)	3.34 (0.52)
fMRI motions (mDVARS)	0.44 (0.25)	0.51 (0.36)	0.40 (0.28)
Bayley-III	Sex, num of females (%)	36/84 (42.86 %)	163/338 (48.22 %)
	Interview age (months)	21.05 (2.83)	18.96 (1.92)
	Cognitive score	10.07 (2.25)	10.19 (2.00)
	Language score	19.50 (5.36)	19.39 (4.81)
	Motor score	19.98 (3.29)	20.72 (3.03)

* TEA, term-equivalent age; GA, gestational age; PMA, post menstrual age.

2.2. MRI acquisition

Infants underwent brain imaging on a 3 T Philips Achieva scanner, using a dedicated neonatal imaging system including customized 32-channel head coil and patient handling system (Hughes et al., 2017). T2-weighted images were obtained using a Turbo Spin Echo sequence in sagittal and axial slice stacks, with parameters: TR/TE= 12000/156 ms, SENSE factor 2.11 (axial) and 2.60 (sagittal), acquisition resolution $0.8 \times 0.8 \times 1.6 \text{ mm}^3$ with a slice overlap of 0.80 mm, reconstructed to 0.5 mm isotropic resolution. Resting-state fMRI was obtained using a gradient-echo echo planar imaging (EPI) sequence, with parameters: TR/TE= 392/38 ms, 2300 volumes, flip angle = 34°, acquired resolution 2.15 mm isotropic. Multi-shell diffusion-weighted MRI (dMRI) was acquired with the following parameters: $b= 0, 400, 1000, \text{ and } 2600 \text{ s/mm}^2$, with spherically uniformly 20, 64, 88, and 128 directions, respectively; TR/TE= 3800/90 ms; multi-band acceleration factor= 4; in-plane resolution= $1.5 \times 1.5 \text{ mm}^2$, and 3 mm slice thickness with 1.5 mm overlap. (Edwards et al., 2022)

2.3. Image preprocessing

The multimodal MRI images from dHCP third release were pre-processed with dedicated minimal preprocessing pipelines including spatial transforms like field map correction, motion correction, distortion correction and spatial registration across multiple modals (Makropoulos et al., 2018; Fitzgibbon et al., 2020), and temporal denoising for rs-fMRI images to remove the structured noise artefacts with spatial independent component analysis (sICA), which has proven to be a powerful tool for separating structured noise from neural signal and is widely used for denoising fMRI in both adults and infants (Smith et al., 2013; Mongerson et al., 2017; Alfaro-Almagro et al., 2018; Fitzgibbon et al., 2020). Based on the minimal preprocessing in current study, a two-stage-process of spatial registration was performed combining one nonlinear warp from native T2w image to the dHCP age-specific template (Bozek et al., 2018) in weeks of PMA and the other linear alignment from the age-specific template to the UNC neonate template space (Shi et al., 2011), using the advanced normalization tools (ANTS, <https://github.com/ANTsX/ANTs>). In addition, a band-pass filter of 0.01–0.08 Hz together with a global signal regression were performed to further control the nonrelevant information and physiological noise in the rs-fMRI signals. The fMRI motions (mDVARS) generated from preprocessing was used as a covariate for generalized linear model.

2.4. Connectivity matrices construction

Using the two-stage-process registration, the UNC infant AAL atlas (Shi et al., 2017) in neonates with 90 parcellations (see *Supplementary Materials, Table S1* for detailed information) was transformed into native space and used as node labeling in both structure and function networks construction, individually. The reconstruction of the diffusion data was performed in native space with DSI-studio. After the generalized q-sampling imaging (GQI) with a diffusion sampling length ratio of 1.25, the whole-brain fiber tracking was conducted with the parameters including the angular cutoff of 60 degrees, step size of 1.0 mm, minimum length of 30 mm, and maximum length of 300 mm. The whole-brain fiber tracking process was performed with the FACT algorithm until 1000,000 streamlines were reconstructed for each individual. The number of streamlines connected between two end regions was normalized by the volume of connected regions, yielding a 90×90 structural connectivity matrix for each individual. For functional connectivity, the Pearson correlations between the paired signals of two regions were calculated and Fisher-z transformed to be the functional connectivity, yielding a 90×90 functional matrix for each individual.

2.5. Structure-function coupling

By combining structural and functional data, structure-function coupling allows for the quantification of how structural connectome constrains spontaneous fluctuations of neural activities. Sparse structural connectivity was firstly transformed into a fully weighted form based on the communication model to avoid the loss of structural information. Then, a multivariate linear regression model was established which combines various predictors to explain more variance when predicting the functional connectivity. The predictors included shortest path length (SPL), communicability (CMC), and Euclidean distance (EUC). They represent different communication strategies: routing, diffusion, and spatial distance, which have been affirmed in many brain network studies (Seguin et al., 2023). And according to research by Esfahlani et al. (2022), these predictors can explain more FC variance compared to other communication measures, and the synergistic effect of multiple predictors leads to increased explanatory power.

Shortest path length denotes the most efficient route between two regions, minimizing the total weight. Communicability (C_{ij}) between node i and node j is defined as the weighted sum of all paths and walks between those nodes (Liu et al., 2022). For a weighted adjacency matrix A (i.e., the structural connectivity matrix), communicability is calculated as $C_{ij} = (\exp(D^{-1/2}AD^{-1/2}))_{ij}$, where D is the degree matrix. Euclidean distance for two brain regions is the straight-line distance between them in the three-dimensional space. Shortest path length was calculated using Brain Connectivity Toolbox (<https://www.nitrc.org/projects/bct/>), a MATLAB toolbox for complex-network analysis.

Concretely, for subject s and region i , we constructed a multiple linear regression model: $fc_{s,i} = \beta_0 + \beta_1 spl_{s,i} + \beta_2 cmc_{s,i} + \beta_3 euc_{s,i}$, where $fc_{s,i}$ is a 90-element vector of functional connectivity in region i (i.e. column i in the FC matrix) predicted by 3 90-element vectors including shortest path length $spl_{s,i}$, communicability $cmc_{s,i}$ and Euclidean distance $euc_{s,i}$. Ordinary least squares method was employed to estimate parameters $\{\beta_0, \beta_1, \beta_2, \beta_3\}$ in the model. In keeping with previous literature, we defined the structure-function coupling index using the R-squared R^2 , the metric for goodness of fit. By doing so, structure-function coupling index for each region of each individual was obtained. The calculation process of structure-function coupling can be found in *Figure S1* in *Supplementary Materials*. Whole-brain analysis was the average of all 90 coupling index resulting in one subject with one value, and network-level analysis was the average of the coupling index in 7 cortical systems (Yeo et al., 2011) and subcortical system.

2.6. Contribution of structural predictors

To better understand which predictor contributes most to the coupling between structure and function, the contributions of these predictors were evaluated. The contribution of a predictor was defined as its regression coefficient in its regression model. To simplify the analysis, the absolute value of the regression coefficient was considered, regardless of its positive or negative effect on the model fitting. After fitting the regression models, a data set with dimensions of $[N_{subject} \times N_{ROI} \times 3]$ was obtained.

The group differences (i.e. three predictor groups: SPL, CMC and EUC) were examined using one-way ANOVA and the Tukey HSD post-hoc test to show pairwise significance. To demonstrate the contribution of each predictor to regional coupling, the proportion of subjects who use the predictor as the most contributing predictor was calculated for each group. Specifically, for each brain region, we need to determine which of the three predictors has the maximum contribution for each subject, and then calculate the percentage of subjects for each predictor across all regions. This resulted in a $[N_{roi} \times 3]$ matrix where each row corresponds to a region, and each column corresponds to one of the predictors (SPL, CMC, or EUC). Then of the three predictors, the most contributing one for each region across subjects was mapped and

visualized (detailed in [Supplementary Materials](#)).

2.7. Developmental trajectory

To map the developmental trajectory of the perinatal structure-function coupling of neonates, subjects were grouped into 10 bins based on PMA, with each bin including 20 individuals, allowing for overlapping PMA ranges. Averaged structure-function coupling index and PMA were calculated for each bin. Then, a smooth function fitting on these 10 data points was performed.

The linear developmental trajectory was also examined for preterm at TEA and full-term by employing a generalized linear regression model. The model included PMA as the independent variable, structure-function coupling index as the dependent variable, and gender and fMRI motions (mDVARs) as possible confounding terms. In a further study, in order to discuss the effect of the extra-uterine exposure time on the linear growth trend, we add GA into the model as an additional confounding term to control for the same intrauterine time for full-term and preterm infants.

2.8. Statistical analysis

Statistical analysis has been used in all four sections of the results. Here, it will be summarized into corresponding four parts.

- (1) **Group differences among three groups.** One-way ANOVA and unpaired two-sided T-test were conducted at whole-brain level to unveil the cross-sectional group difference of coupling among Preterm at birth, at TEA and full-term groups.
- (2) **Longitudinal analysis.** Then, longitudinal analysis was performed with the preterm including 63 infants who had two longitudinal scans from birth to TEA. Group differences were compared using a paired two-sided T-test on the level of both region and network level.
- (3) **Analysis of preterm development.** An unpaired two-sided T-test was applied to compare the differences Preterm at TEA and Full-term groups. The generalized linear regression model was utilized to assess the linear correlation between structure-function coupling index and PMA, incorporating gender and fMRI motions as covariates.
- (4) **Brain-behavior analysis.** PMA and gender were first regressed from structure-function coupling index. Pearson's correlation was then applied to examine the association between the

coupling index and the behavioral outcomes for each brain region.

All analyses, except for the brain-behavior analysis, were corrected for multiple comparisons using the Benjamini-Hochberg method ([Benjamini and Hochberg, 1995](#)) to control the false discovery rate (FDR) at a p-value threshold of 0.05.

3. Results

3.1. Structure-function coupling in infants

The group patterns of structure-function coupling for the preterm at birth, the preterm at term-equivalence and the full-term were illustrated in [Fig. 1a](#). The three spatial distributions of structure-function coupling patterns were quite similar, with relatively lower index in the preterm at birth. The highly coupled regions were located at the medial side of the brain, predominantly associated with areas related to sensory-motor and visual cortical networks ([Fig. 1a](#)). The whole-brain structure-function coupling between the three groups showed a significant difference ([Fig. 1b](#), $F(2,670) = 25.24$, $p = 2.694e-11$), illustrated as high in Preterm at TEA, low in Preterm at birth and middle in full-term.

3.2. Longitudinal analysis of structure-function coupling for preterm infants

Significant longitudinal growth of the coupling index was detected and primarily observed in the bilateral visual cortex, the bilateral cingulate gyrus, the bilateral prefrontal regions, the bilateral temporal cortex, and the left sensorimotor cortex ([Fig. 2a](#)). Based on the brain communities including cortical systems ([Yeo et al., 2011](#)) and subcortical system, the longitudinal growth of the coupling index for each community was extracted and compared, which resulted in significant growths of seven cortical systems except the subcortical network ([Fig. 2b](#)). The largest growth occurred in the visual system (growth percent 70.85 %).

To examine the growth of the coupling index on the individual level, the whole-brain coupling index was calculated for each infant. Note that, for most preterm infants, the development of the coupling index, either increasing or decreasing, crossed the average level of full-term infants' structure-function coupling, which is indicated using the grey dashed line in [Fig. 2c](#).

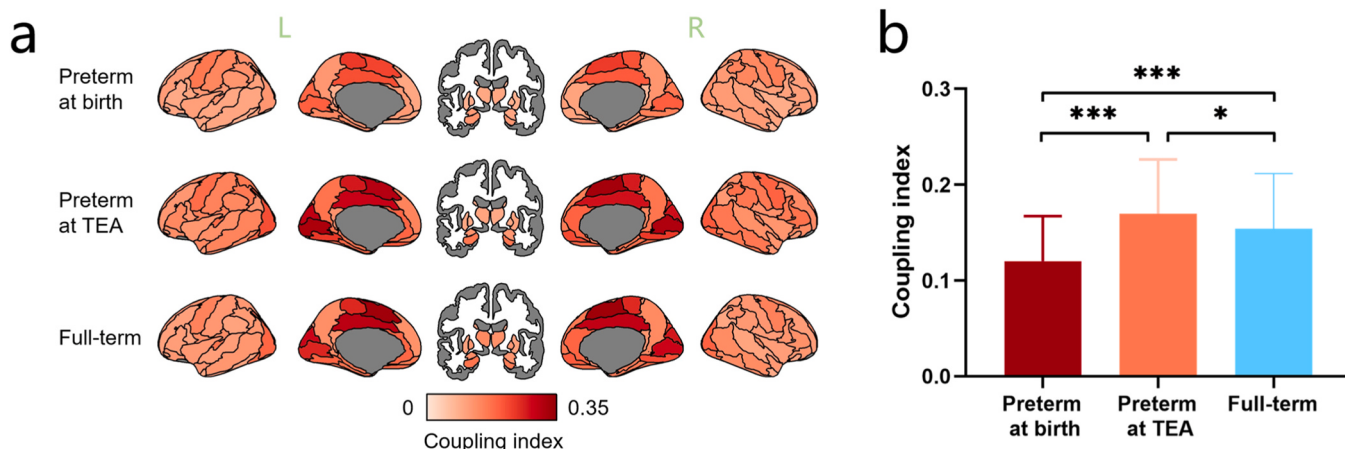


Fig. 1. The mean pattern of structure-function coupling in infants' brains. **a** Spatial distribution of regional coupling obtained by averaging subject data in each group. The middle column shows subcortical regions. **b** The group differences of whole-brain structure-function coupling. Bar charts show mean values and standard deviations of the coupling index for the three subject groups. An unpaired two-sided t-test was employed (p-values: preterm at birth vs preterm at TEA: 1.9e-11; preterm at birth vs full-term: 8.9e-09; preterm at TEA vs full-term: 0.011; FDR corrected; *, **, *** indicates results are significant at $p < 0.05$, $p < 0.01$, and $p < 0.001$).

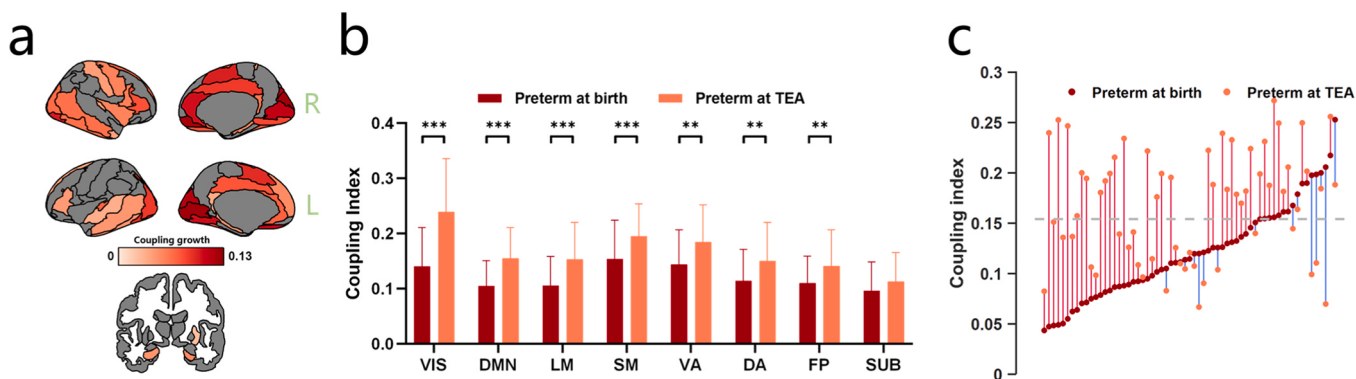


Fig. 2. The growth of structure-function coupling in preterm infants. **a** Growth of regional coupling from birth to term equivalent. A paired two-sided *t*-test was employed. The grey area indicates no significant difference (FDR corrected, $p < 0.05$, detailed in Table S2). **b** The group differences of structure-function coupling for each network (visual (VIS), default mode (DMN), limbic (LM), sensorimotor (SM), ventral attention (VA), dorsal attention (DA), frontoparietal control (FP), and subcortical (SUB) network). The networks are arranged based on the magnitude of inter-group mean difference, with larger differences positioned closer to the Y-axis. A paired two-sided *t*-test was employed (FDR corrected; *, **, *** indicates results are significant at $p < 0.05$, $p < 0.01$, and $p < 0.001$). **c** The growth of whole-brain coupling index for each infant. Each line represents the growth of structure-function coupling in an individual. The red line represents an increase, while the blue line represents a decrease. The grey dashed line represents the average whole-brain coupling index of full-term group.

3.3. Overgrowth of structure-function coupling in preterm infants

In this section, we conducted a comparative analysis of structure-function coupling patterns between full-term infants and preterm

infants at TEA to identify distinct coupling characteristics and developmental trajectories between the two groups. Group differences were first compared between Preterm at TEA and Full-term on the level of region and network. For brain regions, the coupling differences were

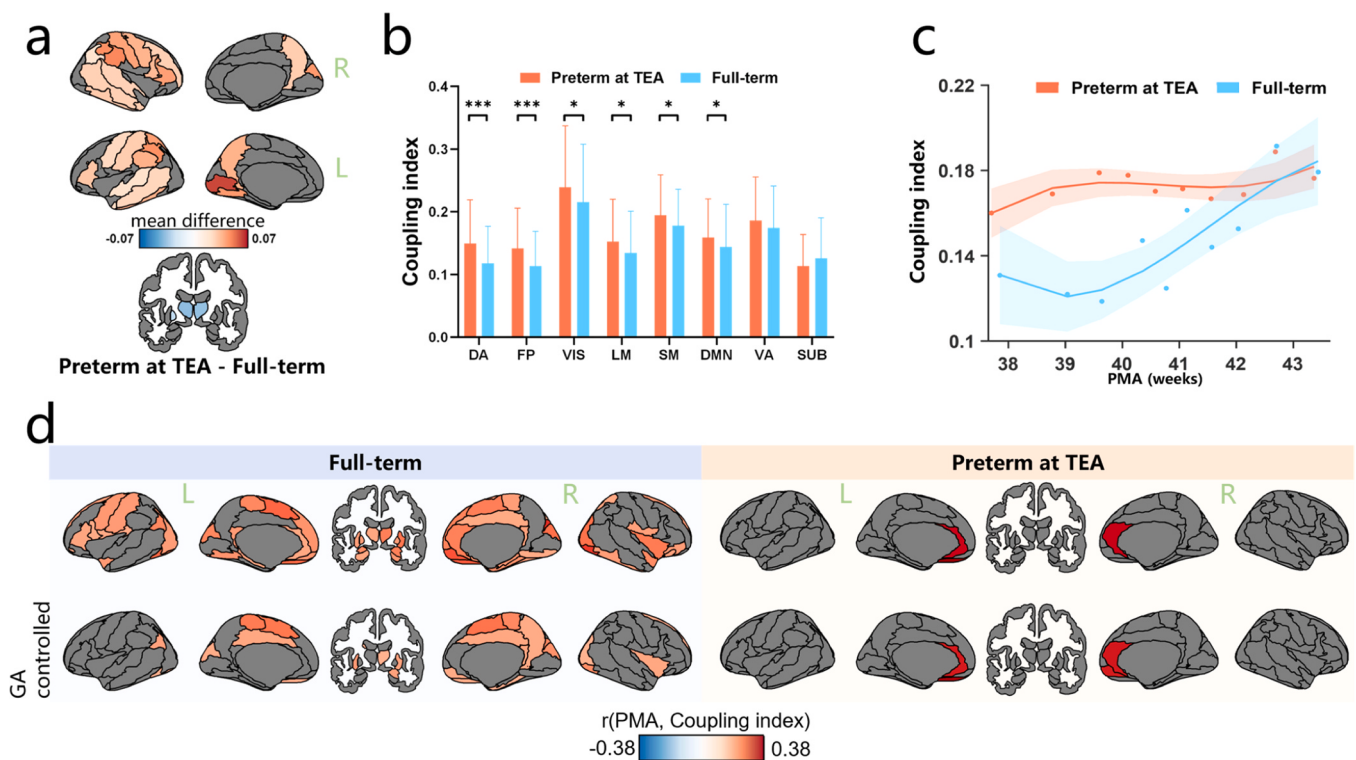


Fig. 3. Development of structure-function coupling in preterm and full-term infants. **a** The group differences between preterm at TEA and full-term on the regional level. An unpaired two-sided *t*-test was employed. The grey area indicates no significant difference (FDR corrected, $p < 0.05$, detailed in Table S3), and the red and blue areas indicate the mean difference in structure-function coupling index. **b** The group differences of structure-function coupling for each network (visual (VIS), default mode (DMN), limbic (LM), sensorimotor (SM), ventral attention (VA), dorsal attention (DA), frontoparietal control (FP), and subcortical (SUB) network). The networks are arranged based on the magnitude of inter-group mean difference, with larger differences positioned closer to the Y-axis. An unpaired two-sided *t*-test was employed (FDR corrected; *, **, *** indicates results are significant at $p < 0.05$, $p < 0.01$, and $p < 0.001$). **c** The developmental trajectory of whole-brain structure-function coupling. Infants in each group were grouped into 10 bins based on PMA. Each point represents the mean value of a bin. The shaded envelope denotes the 95 % confidence interval. The lines were smoothed to better display the trends. **d** Linear developmental trend of structure-function coupling for preterm and full-term infants. The *r*-values from Pearson's correlation between the coupling index and PMA are shown on the brain maps. In the first row, gender and fMRI motions were regressed from structure-function coupling index. GA was then controlled as a covariate in the following row. The grey area indicates no significant linear correlation in the generalized linear regression model (FDR corrected, $p < 0.05$, detailed in Table S4 and S5 for full-term group and Table S6 for preterm group).

highest in the left medial occipital lobe, right supramarginal gyrus and bilateral inferior parietal lobules (IPL) (Fig. 3a). For brain networks, the dorsal attention and frontoparietal network exhibited the greatest group differences, with the visual network closely following (Fig. 3b). In this case, higher coupling of dorsal attentional network was widely presented on all regions, and the frontoparietal network was mainly driven by IPL. According to these findings and the observed increase in structure-function coupling from longitudinal data in preterm infants, it is reasonable to infer an overgrowth phenomenon in preterm.

Then, the developmental trajectories of the two groups were investigated by binning infants according to their PMA. Fig. 3c illustrates the developmental trajectory of whole-brain structure-function coupling. From 38 weeks to 43 weeks, a noticeable reduction in the structure-function coupling differences between the two groups was evident. The same analysis was repeated in each network and observed a similar pattern in all cortical networks (see [Supplementary Materials, Figure S3](#)). Considering the developmental trajectory of full-term infants as a baseline, the decreasing differences can be interpreted as preterm infants undergoing developmental correction.

To assess how the developmental trend of global growth varies in brain regions and whether it is statistically valid, linear growth trends at the regional level were assessed. On the regional level, full-term infants exhibited a greater number of regions with significant linear growth trends, primarily in the occipital lobe, parietal lobe, and medial prefrontal cortex. In contrast, preterm infants only showed significant linear growth trends in the regions belonging to the default mode network, including the left superior frontal gyrus with medial orbital

part and the anterior cingulate and paracingulate gyri on both sides. Furthermore, by including GA as another covariate in a repeated analysis, we controlled for differences in intrauterine growth time, focusing solely on the impact of the extrauterine environment on structure-function coupling (Fig. 3d). The results showed contrasting outcomes between full-term and preterm infants: the number of significant regions in full-term infants decreased, while in preterm infants, the trend of linear growth of the medial orbital of superior frontal gyrus, shifted from non-significant to significant.

3.4. Linking structure-function coupling at birth to later behavioral outcomes

In the previous section, we identified the overgrowth of structure-function coupling in preterm infants. Further, we were curious about whether early structure-function coupling relates to or even predicts later behavioral outcomes. To answer this question, we analyzed data from full-term and preterm infants at TEA, specifically focusing on their structure-function coupling at scan and these behavioral outcomes at age 20 months. Significant correlations were observed in both groups between their coupling index and the cognitive and language scores, but no significant region was observed for motor scores. Noteworthy, negative associations for preterm and positive associations for full-term were identified in the analysis (Fig. 4a and d). The brain regions with the maximum positive and negative correlations in both groups are circled and displayed in the scatter plots as shown in Fig. 4. The right inferior parietal lobule was observed to be more strongly associated with the

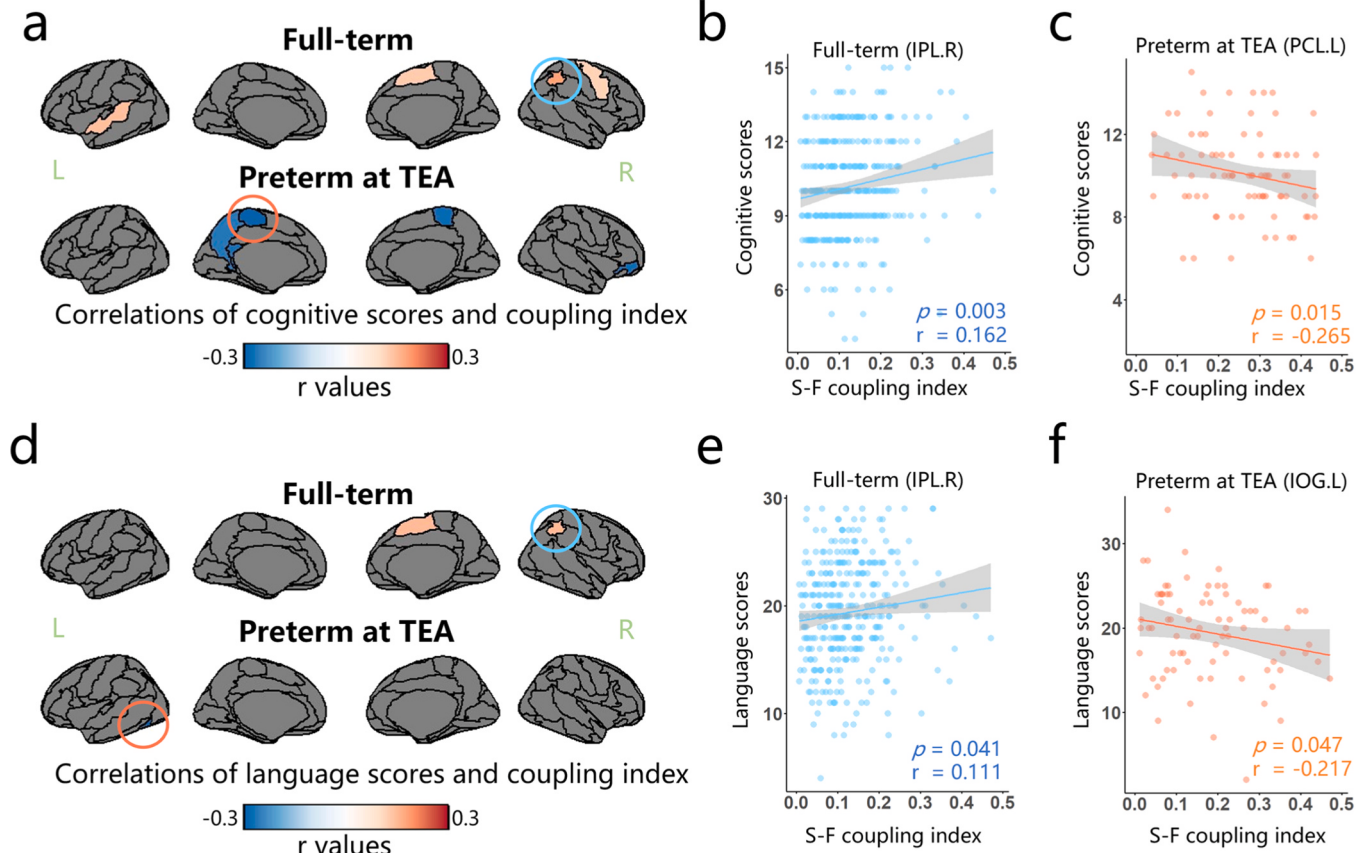


Fig. 4. Correlations between the coupling index at scan and the cognitive and language performances at later ages. The r-values from Pearson's correlation between structure-function coupling index and the cognitive (a) and language (d) scores are displayed on the brain maps. The grey area indicates no significant correlation ($p < 0.05$, detailed in [Table S7 and S8](#)). (b) and (c) show two regions with the maximum correlation between the coupling index and cognitive scores for full-term and preterm groups, respectively, which are circled with the same color in (a). (e) and (f) show two regions with the maximum correlation between the coupling index and language scores for full-term and preterm groups, respectively, which are circled with the same color in (d). Each point represents an individual. The shaded envelope denotes the 95 % confidence interval. IPL.R, the right inferior parietal; PCL.L, the left paracentral lobule; IOG.L, the left inferior occipital gyrus.

coupling index in full-term group for both cognitive and language scores. In preterm group, strong associations were observed in the left paracentral lobule (PCL.L) for cognitive scores and left inferior occipital gyrus (IOG.L) for language scores.

4. Discussion

Using multimodal neuroimaging data from newborns, we investigated structure-function coupling in preterm and full-term infants. Our study examined several key findings. Firstly, typical structure-function coupling was observed in preterm brains, displaying a similar distribution but higher coupling than the full-term group. Secondly, the coupling in preterm infants exceeded that of full-term infants, indicating an overgrowth from birth to equivalent postmenstrual ages. Over time, this gap gradually diminished with brain development. Furthermore, our study revealed that the overgrowth observed in preterm had a negative impact on later behavioral outcomes.

During the perinatal period, the newborn brain exhibits a distinct pattern of structure-function coupling characterized by hemispheric symmetry, with stronger coupling in unimodal cortices and weaker coupling in transmodal cortices. This distribution has been documented in recent studies (Prete and Van De Ville, 2019; Vázquez-Rodríguez et al., 2019; Suárez et al., 2020). One explanation for this pattern is that the rapid expansion of the cortex releases related regions from early sensorimotor hierarchy, resulting in significant variance and weaker structure-function relationships in transmodal regions (Buckner and Krienen, 2013). The nuanced hierarchical coupling observed in the lateral cortex reflects functional specialization (Baum et al., 2020). However, due to incomplete myelination and the consequent lack of extensive neural circuitry, the coupling hierarchy in infants is less refined compared to that in adolescents. Furthermore, the subcortical system does not exhibit the high-level coupling observed in adult brains (Gu et al., 2021), aligning with theories that prioritize the development of primary functions (Brenner et al., 2021).

From birth to term-equivalent age, structure-function coupling in preterm infants shows widespread growth across most regions of the brain and all cortical networks (Fig. 2a and b). Coupling in regions associated with visual function, such as the medial occipital lobe, grew the most, aligning with expected developmental trajectories of experience-dependent plasticity during early postnatal visual system maturation. Significant changes in the frontoparietal network may be driven by the inferior frontal gyrus. This region, along with the subcortical regions, is associated with higher cognitive functions, and the slight changes in these regions align with the theory of prioritized development of primary functions. Additionally, extensive coupling growth in cortical regions resulted in significantly higher coupling than in the full-term group, particularly in the lateral brain. Using full-term infants as a baseline, this higher coupling is considered as the overgrowth of structure-function coupling.

The overgrowth of structure-function coupling observed in preterm infants can be partly explained by myelination. Myelination during this period plays a crucial role in neural signal transmission, accelerating signal conduction speed, protecting axons, and conserving energy, which ensures efficient and precise local communications and facilitates global resource allocation (Fields, 2015; Qiu et al., 2015). The myelination of neural fibers, characterized by high fidelity and efficiency in information transmission, can offer deeper insights into the heterogeneity of structure-function coupling (Vandewouw et al., 2021). Evidence from the adult brain has demonstrated that structure-function coupling is positively correlated with intracortical myelin content (Fotiadis et al., 2023). Meanwhile, a stereology study of neonatal myelination found myelinated fiber length density is low in visual, sensorimotor, and prefrontal regions at birth but increases rapidly during infancy (Miller et al., 2012). The process of myelination parallels the structure-function coupling observed in our results (Fig. 2a). Notably, preterm infants experience more extra-uterine time than term infants and receive more

sensory and visual inputs, leading to an acceleration of the myelination process. This may directly cause higher coupling in preterm infants.

From the perspective of information transfer, the overgrowth of structure-function coupling in preterm infants limits functional flexibility and disrupts the strategy of resource allocation. Structure-function coupling emphasizes the fidelity of information transmission, but higher coupling implies a higher degree of restriction of function by structure, thereby reducing the efficiency of information exchange. Our study identified widespread and rapid growth of structure-function coupling in the cortical regions of preterm infants at both group and individual levels, resulting in an overgrowth of the coupling after the 37-week postmenstrual age. Higher coupling in unimodal regions ensures the fidelity of information transmission in brain networks, leading to behavioral consequences (Suárez et al., 2020). The increased coupling observed in unimodal regions from preterm brains, such as visual and sensorimotor networks, can be explained by the preterm infants receiving more sensory inputs. While lower coupling in transmodal regions supports functional flexibility and dynamic recruitment during diverse task demands (Yeo et al., 2014). Interestingly, we observed the overgrowth of coupling in transmodal association networks, especially in dorsal attention and frontoparietal networks. The overgrowth of coupling may be associated with global resource allocation during the process of myelination. Prematurity disrupts the pre-established strategy, leading to widespread increases in coupling across the whole brain. This process contributes to the delayed brain development, consistent with the little progress of myelination observed in preterm infants after 34 weeks of gestation (Sie et al., 1997).

Despite the higher coupling strength observed in preterm brains due to overgrowth, ongoing corrective mechanisms are actively engaged, bringing the development of structure-function coupling back on track toward the normal trajectory. The investigation into the developmental trajectory of structure-function coupling indicates that the overgrowth in cortical networks appears to be physiologically corrected after PMA 40 weeks, resulting in a gradual reduction of the gap between preterm and full-term infants. The correction is analogous to the catch-up growth observed in preterm infants and children such as in weight and head size development (Lee and Hayes, 2015; Durá-Travé et al., 2020). The emergence of the correction mechanism appears to be linked to rapid brain development optimizing structure-function relationships to enhance overall information transmission efficiency. Specifically, the correction observed in unimodal regions reflects a strategic resource allocation strategy, involving a reduction in coupling strength to minimize metabolic energy consumption (Collin et al., 2013). These dynamic processes collectively highlight the brain's inherent capacity for self-optimization in support of efficient and precise information processing.

The developmental trajectory of structure-function coupling in preterm infants is highly sensitive to the extra-uterine environment, making it more complex. Early extra-uterine exposure of preterm infants alters their brains in the developmental rates of white and gray matter, resulting in an immature structural framework and delayed development (Brossard-Racine et al., 2019; Grotheer et al., 2023). Research on fMRI confirms that preterm infants exhibit stronger functional connectivity in sensory-related networks (De Asis-Cruz et al., 2020). Consistent with these findings, abnormal development of structure-function coupling was captured in our study by correlating post-menstrual ages and the coupling index. Specifically, regions exhibiting a significant linear growth trend were fewer in preterm infants compared to full-term, indicating that the developmental trajectory of the former is more complex rather than merely following a simple linear growth pattern. This complex development was supposed to be partly attributed to early extra-uterine exposure because the linear growth trends were observed in more regions in preterm and fewer regions in full-term after controlling their gestational ages. Notably, in preterm infants, the regions exhibiting a linear growth trend all belong to the default mode network, and this association is even stronger than in all regions of

full-term infants. However, the default mode network is supposed to be established through childhood with associated higher cognitive functions emerge (Gao et al., 2015). The evidence provided by Yu et al. (2023) also suggests that in full-term infants, the default mode network emerges alongside increased regional blood flow before age 2. So, we suspect that the linear growth in certain regions of the default mode network in preterm infants may indicate an early entrance into the growth period observed in full-term infants.

The variance in later behavioral outcomes can be partly explained by early regional coupling. Existing literature provides evidence that preterm birth alters the structural wiring of infants' brains, impacting their behavioral performances like cognition and language (Rogers et al., 2018; Ji et al., 2023; Sun et al., 2023). Consistent with these findings, our study revealed that structure-function coupling was associated with behavioral outcomes, showing negative correlations in preterm infants and positive correlations in full-term infants. IPL is a key neural substrate underlying diverse mental processes—from basic attention to language and social cognition—that define human interactions (Kernbach et al., 2018). Structure-function coupling in this region may predict later cognitive and language outcomes in full-term infants. Furthermore, structure-function coupling is thought to be strongly associated with cognition, whether in adults, children, or the elderly. Fotiadis et al. discussed their relationships, arguing that structure-function coupling could be critical in identifying the point of transition from cognitive resilience to cognitive impairment (Fotiadis et al., 2024). For example, studies involving individuals with cognitive impairments have consistently demonstrated a reduced integrity of structural connectivity in both children and adult populations (van den Heuvel et al., 2013b; Thompson et al., 2016). This reduction is hypothesized to contribute to reduced complexity in functional interactions, consequently leading to a strong structure-function coupling. Although our analysis did not address cognitive impairment, a slight association between cognition and coupling was captured from the results of higher r-values and significance, and more significant brain regions observed in cognitive assessments rather than language and motor (Fig. 4a and d). Interestingly, the coupling correlated with cognitive and language scores but not motor scores. A reasonable explanation is that the environmental factors dominate the brain development during the considerable time gap between scanning and behavioral assessments. During this time gap, motor learning tends to be most pronounced, followed by language, while cognitive development typically occurs at a later stage. This aligns with the developmental hierarchy of functional networks, from primary sensorimotor functions to higher cognitive functions (Ouyang et al., 2019), and aligns with a gradual increase in the correlation between early coupling and corresponding behavioral outcomes (no correlation - maximum correlation $-0.217/0.111$ - maximum correlation $-0.265/0.162$, preterm/full-term, Fig. 4). It is possible that more robust correlations between neonatal structure-function coupling and behavioral outcomes could have been identified had MRI scans been available when assessing behavioral outcomes. While this limitation is regrettable, it is noteworthy that our findings indicate that structure-function coupling is a sensitive measure for evaluating cognitive performance.

Significant regions in preterm group are notably as well. The PCL region has been linked to motor control of the contralateral lower limb (Laplane et al., 1977). Motor and cognitive functions are thought to be closely related during development (Leisman et al., 2016), as researchers routinely assess cognition in pre-verbal infants through their movements, such as gaze shifts, head turns, or reaching for objects. On the other hand, higher coupling in PCL means higher information communicating with the whole brain, suggesting that active participation in information processing in this region has a positive effect on later cognition. The IOG region is anatomically associated with the white matter tract Inferior Fronto-Occipital Fasciculus (IFOF) and it serves as the origin of the deep ventral subcomponent of the IFOF (Martino et al., 2010). Recent findings have revealed the role of this subcomponent in

language processing, supporting access to familiar semantic units (Eze et al., 2024). This fits the scenario of early language acquisition, with repetition of vocabularies. Regarding the result of opposite correlations observed between groups, it may reflect region-specific structure-function coupling, and it could simply be a coincidence that opposite results were observed in these regions considering the few numbers of significant regions. Moreover, the regions showing opposite results are not the same, which further complicates direct comparisons between them. We also conducted correlations between whole-brain coupling and these behavioral outcomes, but no significant associations were found in both groups.

Several constraints warrant further consideration. Firstly, shortest path length as a measure of communication in the brain network has been questioned by certain studies. Employing shortest path for communication necessitates a comprehensive understanding of its shortest path structure (Goñi et al., 2014; Avena-Koenigsberger et al., 2019), which is biologically implausible due to the complexity of network connections. The results of the contributions of predictors used in this study corroborated the previous findings. Shortest path contributed less than the other two predictors (Figure S2), suggesting that in cortical regions, information transfer was not absolutely efficient, but was dominated by a strategy of diffusion, where information transfer was traded off with an energetic cost (Seguin et al., 2023). Consequently, further research is imperative to explore alternative communication strategies. Secondly, despite the large sample size in studies on infant neuroimaging, the heightened sensitivity of preterm brains to the environment results in more complex developmental outcomes and greater individual differences (Dimitrova et al., 2021). The developmental patterns for preterm infants may not reflect the broader population. Thirdly, the lack of MRI scans during behavioral assessments poses a limitation. There is a long time gap in brain-behavior analysis, which is weak in explaining the association between coupling and cognition. The relationship between coupling differences and cognitive differences in preterm and term infants is still not clear. Finally, given the limited sample size, socioeconomic conditions like home environment and parenting style are not explored in the brain-behavioral analyses. The period between MRI scanning and behavioral assessment is primarily influenced by environmental factors, which may affect behavioral outcomes. Therefore, exploring the moderating role of the environment in brain-behavior interactions is both an interesting and meaningful research direction. Our future studies will focus on this aspect.

In summary, the immaturity of the brain is very sensitive and vulnerable to explosive environmental inputs. The preterm infant brain possesses a low level of structure-function coupling at birth and goes through overgrowth to the term equivalent age. This overgrowth of brain structure-function coupling for preterm infants was verified to be negatively correlated with later behavioral outcomes. Collectively, our findings reveal the dynamic developmental trajectory of brain structure-function relationships during infancy, offering new insights into the information transmission processes and developmental patterns of the early-life brain.

CRediT authorship contribution statement

Wang Rong: Writing – review & editing, Writing – original draft, Visualization, Software, Investigation, Formal analysis, Conceptualization. **Fang Tianyu:** Writing – review & editing, Validation, Investigation. **Zhang Yue:** Writing – review & editing, Validation. **Cheng Yue:** Funding acquisition. **Wang Chunfang:** Funding acquisition. **Chen Yuanyuan:** Writing – review & editing, Supervision, Project administration, Funding acquisition, Conceptualization. **Fan Qiuyun:** Project administration, Funding acquisition, Conceptualization. **Zhao Xin:** Project administration, Conceptualization. **Ming Dong:** Project administration.

Declaration of Competing Interest

The authors declare that they have no known competing financial interests or personal relationships that could have appeared to influence the work reported in this paper.

Acknowledgments

This work was supported by the National Key Research and Development Program of China (No. 2023YFF1204300), National Natural Science Foundation of China awarded to Yuanyuan Chen (No. 82202249), Qiuyun Fan (No. 82071994), and Chunfang Wang (No. 82102652), Tianjin Health Research Project awarded to Yue Cheng (No. TJWJ2023XK012), and Tianjin Natural Science Foundation awarded to Yue Cheng (No. 21JCYBJC01290).

Data statement

Metadata for all sample used in this study was sourced from the third release of Developing Human Connectome Project (dHCP, <https://www.developingconnectome.org/>), a substantial open science investigation into infant brain development.

Appendix A. Supporting information

Supplementary data associated with this article can be found in the online version at [doi:10.1016/j.dcn.2025.101535](https://doi.org/10.1016/j.dcn.2025.101535).

References

- Alfaro-Almagro, F., Jenkinson, M., Bangerter, N.K., Andersson, J.L., Griffanti, L., Douaud, G., Sotiropoulos, S.N., Jbabdi, S., Hernandez-Fernandez, M., Vallee, E., 2018. Image processing and quality control for the first 10,000 brain imaging datasets from UK Biobank. *Neuroimage* 166, 400–424. <https://doi.org/10.1016/j.neuroimage.2017.10.034>.
- Avena-Koenigsberger, A., Yan, X., Kolchinsky, A., van den Heuvel, M.P., Hagmann, P., Sporns, O., 2019. A spectrum of routing strategies for brain networks. *PLoS Comput. Biol.* 15, e1006833. <https://doi.org/10.1371/journal.pcbi.1006833>.
- Baum, G.L., Cui, Z., Roalf, D.R., Ciric, R., Betzel, R.F., Larsen, B., Cieslak, M., Cook, P.A., Xia, C.H., Moore, T.M., Ruparel, K., Oathes, D.J., Alexander-Bloch, A.F., Shinohara, R.T., Raznahan, A., Gur, R.E., Gur, R.C., Bassett, D.S., Satterthwaite, T.D., 2020. Development of structure-function coupling in human brain networks during youth. *Proc. Natl. Acad. Sci. USA* 117, 771–778. <https://doi.org/10.1073/pnas.1912034117>.
- Benjamini, Y., Hochberg, Y., 1995. Controlling the false discovery rate: a practical and powerful approach to multiple testing. *J. R. Stat. Soc.: Ser. B (Methodol.)* 57, 289–300. <https://doi.org/10.1111/j.2517-6161.1995.tb02031.x>.
- Boardman, J.P., Counsell, S.J., 2020. Invited review: factors associated with atypical brain development in preterm infants: insights from magnetic resonance imaging. *Neuropathol. Appl. Neurobiol.* 46, 413–421. <https://doi.org/10.1111/nan.12589>.
- Bozek, J., et al., 2018. Construction of a neonatal cortical surface atlas using multimodal surface matching in the developing human connectome project. *Neuroimage* 179, 11–29. <https://doi.org/10.1016/j.neuroimage.2018.06.018>.
- Brenner, R.G., Wheelock, M.D., Neil, J.J., Smyser, C.D., 2021. Structural and functional connectivity in premature neonates. *Semin. Perinatol.* 45, 151473. <https://doi.org/10.1016/j.semperi.2021.151473>.
- Brossard-Racine, M., McCarter, R., Murnick, J., Tinkleman, L., Vezina, G., Limperopoulos, C., 2019. Early extra-uterine exposure alters regional cerebellar growth in infants born preterm. *NeuroImage: Clin.* 21, 101646. <https://doi.org/10.1016/j.nicl.2018.101646>.
- Buckner, R.L., Krienen, F.M., 2013. The evolution of distributed association networks in the human brain. *Trends Cogn. Sci.* 17, 648–665. <https://doi.org/10.1016/j.tics.2013.09.017>.
- Ciarrusta, J., Christiaens, D., Fitzgibbon, S.P., Dimitrova, R., Hutter, J., Hughes, E., Duff, E., Price, A.N., Cordero-Grande, L., Tournier, J.D., Rueckert, D., Hajnal, J.V., Arichi, T., McAlonan, G., Edwards, A.D., Bataille, D., 2022. The developing brain structural and functional connectome fingerprint. *Dev. Cogn. Neurosci.* 55, 101117. <https://doi.org/10.1016/j.dcn.2022.101117>.
- Collin, G., Sporns, O., Mandl, R.C.W., van den Heuvel, M.P., 2013. Structural and functional aspects relating to cost and benefit of rich club organization in the human cerebral cortex. *Cereb. Cortex* 24, 2258–2267. <https://doi.org/10.1093/cercor/bht064>.
- Collin, G., Scholtens, L.H., Kahn, R.S., Hillegers, M.H.J., van den Heuvel, M.P., 2017. Affected anatomical rich club and structural-functional coupling in young offspring of schizophrenia and bipolar disorder patients. *Biol. Psychiatr.* 82, 746–755. <https://doi.org/10.1016/j.biopsych.2017.06.013>.
- Dai, Z.J., Lin, Q.X., Li, T., Wang, X., Yuan, H.S., Yu, X., He, Y., Wang, H.L., 2019. Disrupted structural and functional brain networks in Alzheimer's disease. *Neurobiol. Aging* 75, 71–82. <https://doi.org/10.1016/j.neurobiolaging.2018.11.005>.
- Damaraju, E., Phillips, J., Lowe, J.R., Ohls, R., Calhoun, V.D., Caprihan, A., 2010. Resting-state functional connectivity differences in premature children. *Front. Syst. Neurosci.* 4. <https://doi.org/10.3389/fnsys.2010.00023>.
- De Asis-Cruz, J., Kapse, K., Basu, S.K., Said, M., Scheinost, D., Murnick, J., Chang, T., du Plessis, A., Limperopoulos, C., 2020. Functional brain connectivity in ex utero premature infants compared to in utero fetuses. *Neuroimage* 219, 117043. <https://doi.org/10.1016/j.neuroimage.2020.117043>.
- van den Heuvel, M.P., Sporns, O., Collin, G., Scheewe, T., Mandl, R.C., Cahn, W., Goni, J., Hulshoff Pol, H.E., Kahn, R.S., 2013b. Abnormal rich club organization and functional brain dynamics in schizophrenia. *JAMA Psychiatry* 70, 783–792. <https://doi.org/10.1001/jamapsychiatry.2013.1328>.
- van den Heuvel, M.P., Sporns, O., Collin, G., Scheewe, T., Mandl, R.C.W., Cahn, W., Goni, J., Pol, H.E.H., Kahn, R.S., 2013a. Abnormal rich club organization and functional brain dynamics in schizophrenia. *Jama Psychiatry* 70, 783–792. <https://doi.org/10.1001/jamapsychiatry.2013.1328>.
- Dimitrova, R., et al., 2021. Preterm birth alters the development of cortical microstructure and morphology at term-equivalent age. *Neuroimage* 243, 118488. <https://doi.org/10.1016/j.neuroimage.2021.118488>.
- Durá-Travé, T., Martín-García, San, Gallinas-Victoriano, I., Chueca-Guindulain, F., Berrada-Zubiri S, M.J., 2020. Catch-up growth and associated factors in very low birth weight infants. *An. De. Pedia ía (Engl. Ed.)* 93, 282–288. <https://doi.org/10.1016/j.anpede.2019.06.007>.
- Edwards, A.D., Rueckert, D., Smith, S.M., Abo Seada, S., Alansary, A., Almalbis, J., Allsop, J., Andersson, J., Arichi, T., Arulkumaran, S., 2022. The developing human connectome project neonatal data release. *Front. Neurosci.* 16, 886772. <https://doi.org/10.3389/fnins.2022.886772>.
- Esfahlani, F.Z., Faskowitz, J., Slack, J., Misic, B., Betzel, R.F., 2022. Local structure-function relationships in human brain networks across the lifespan. *Nat. Commun.* 13. <https://doi.org/10.1038/s41467-022-29770-y>.
- Eyre, M., et al., 2021. The developing human connectome project: typical and disrupted perinatal functional connectivity. *Brain* 144, 2199–2213. <https://doi.org/10.1093/brain/awab118>.
- Eze, P., Omorionmwani, E., Cummine, J., 2024. Moving towards an understanding of the role of the inferior fronto-occipital fasciculus in language processing. *Neurosci. -Basel* 5, 39–58. <https://doi.org/10.3390/neurosci5010003>.
- Fields, R.D., 2015. A new mechanism of nervous system plasticity: activity-dependent myelination. *Nat. Rev. Neurosci.* 16, 756–767. <https://doi.org/10.1038/nrn4023>.
- Fitzgibbon, S.P., et al., 2020. The developing human connectome project (dHCP) automated resting-state functional processing framework for newborn infants. *NeuroImage* 223, 117303. <https://doi.org/10.1016/j.neuroimage.2020.117303>.
- Fotiadis, P., Cieslak, M., He, X.S., Caciagli, L., Ouellet, M., Satterthwaite, T.D., Shinohara, R.T., Bassett, D.S., 2023. Myelination and excitation-inhibition balance synergistically shape structure-function coupling across the human cortex. *ARTN 6115 Nat. Commun.* 14. <https://doi.org/10.1038/s41467-023-41686-9>.
- Fotiadis, P., Parkes, L., Davis, K.A., Satterthwaite, T.D., Shinohara, R.T., Bassett, D.S., 2024. Structure-function coupling in macroscale human brain networks. *Nat. Rev. Neurosci.* 25, 688–704. <https://doi.org/10.1038/s41583-024-00846-6>.
- França, L.G.S., et al., 2024. Neonatal brain dynamic functional connectivity in term and preterm infants and its association with early childhood neurodevelopment. *ARTN 16 Nat. Commun.* 15. <https://doi.org/10.1038/s41467-023-44050-z>.
- Gao, W., Alcauter, S., Elton, A., Hernandez-Castillo, C.R., Smith, J.K., Ramirez, J., Lin, W., 2015. Functional network development during the first year: relative sequence and socioeconomic correlations. *Cereb. cortex* 25, 2919–2928. <https://doi.org/10.1093/cercor/bhu088>.
- Girault, J.B., Munsell, B.C., Puechmaille, D., Goldman, B.D., Prieto, J.C., Styner, M., Gilmore, J.H., 2019. White matter connectomes at birth accurately predict cognitive abilities at age 2. *Neuroimage* 192, 145–155. <https://doi.org/10.1016/j.neuroimage.2019.02.060>.
- Goñi, J., Van Den Heuvel, M.P., Avena-Koenigsberger, A., Velez de Mendizabal, N., Betzel, R.F., Griffa, A., Hagmann, P., Corominas-Murtra, B., Thiran, J.-P., Sporns, O., 2014. Resting-brain functional connectivity predicted by analytic measures of network communication. *Proc. Natl. Acad. Sci.* 111, 833–838. <https://doi.org/10.1073/pnas.1315529111>.
- Griffa, A., Amico, E., Liegeois, R., Van De Ville, D., Preti, M.G., 2022. Brain structure-function coupling provides signatures for task decoding and individual fingerprinting. *NeuroImage* 250, 118970. <https://doi.org/10.1016/j.neuroimage.2022.118970>.
- Grotheer, M., Bloom, D., Kruper, J., Richie-Halford, A., Zika, S., Aguilera González, V.A., Yeatman, J.D., Grill-Spector, K., Rokem, A., 2023. Human white matter myelinates faster in utero than ex utero. *Proc. Natl. Acad. Sci.* 120, e2303491120. <https://doi.org/10.1073/pnas.2303491120>.
- Gu, Z., Jamison, K.W., Sabuncu, M.R., Kuceyeski, A., 2021. Heritability and interindividual variability of regional structure-function coupling. *Nat. Commun.* 12, 4894. <https://doi.org/10.1038/s41467-021-25184-4>.
- Honey, C.J., Sporns, O., Cammoun, L., Gigandet, X., Thiran, J.P., Meuli, R., Hagmann, P., 2009. Predicting human resting-state functional connectivity from structural connectivity. *Proc. Natl. Acad. Sci. USA* 106, 2035–2040. <https://doi.org/10.1073/pnas.0811168106>.
- Hu, D., Wang, F., Zhang, H., Wu, Z., Zhou, Z., Li, G., Wang, L., Lin, W., Li, G., Consortium, U.U.B.C.P., 2022. Existence of functional connectome fingerprint during infancy and its stability over months. *J. Neurosci.* 42, 377–389. <https://doi.org/10.1523/JNEUROSCI.0480-21.2021>.

- Hughes, E.J., Winchman, T., Padorno, F., Teixeira, R., Wurie, J., Sharma, M., Fox, M., Hutter, J., Cordero-Grande, L., Price, A.N., 2017. A dedicated neonatal brain imaging system. *Magn. Reson. Med.* 78, 794–804. <https://doi.org/10.1002/mrm.26462>.
- Ji, W., Li, G., Jiang, F., Zhang, Y., Wu, F., Zhang, W., Hu, Y., Wang, J., Wei, X., Li, Y., 2023. Preterm birth associated alterations in brain structure, cognitive functioning and behavior in children from the ABCD dataset. *Psychol. Med.* 1–10. <https://doi.org/10.1017/S0033291723001757>.
- Kernbach, J.M., Yeo, B.T.T., Smallwood, J., Margulies, D.S., Thiebaut De Schotten, M., Walter, H., Sabuncu, M.R., Holmes, A.J., Gramfort, A., Varoquaux, G., Thirion, B., Bzdok, D., 2018. Subspecialization within default mode nodes characterized in 10,000 UK biobank participants. *P. Natl. Acad. Sci. USA* 115, 12295–12300. <https://doi.org/10.1073/pnas.1804876115>.
- Kulik, S.D., Nauta, I.M., Tewarie, P., Koubiy, I., van Dellen, E., Ruet, A., Meijer, K.A., de Jong, B.A., Stam, C.J., Hillebrand, A., Geurts, J.J.G., Douw, L., Schoonheim, M.M., 2022. Structure-function coupling as a correlate and potential biomarker of cognitive impairment in multiple sclerosis. *Netw. Neurosci.* 6, 339–356. https://doi.org/10.1162/netn_a_00226.
- Laplane, D., Talairach, J., Meiningher, V., Bancaud, J., Orgogozo, J.M., 1977. Clinical consequences of corticectomies involving the supplementary motor area in man. *J. Neurol. Sci.* 34, 301–314. [https://doi.org/10.1016/0022-510X\(77\)90148-4](https://doi.org/10.1016/0022-510X(77)90148-4).
- Lee, K.A., Hayes, B.C., 2015. Head size and growth in the very preterm infant: a literature review. *Res. Rep. Neonatol.* 5 1–7. <https://doi.org/10.2147/RRN.S74449>.
- Leisman, G., Moustafa, A.A., Shafir, T., 2016. Thinking, walking, talking: integratory motor and cognitive brain function. ARTN 94 *Front Public Health* 4. <https://doi.org/10.3389/fpubh.2016.00094>.
- Liu, Z.Q., Vázquez-Rodríguez, B., Spreng, R.N., Bernhardt, B.C., Betzel, R.F., Misic, B., 2022. Time-resolved structure-function coupling in brain networks. *Commun. Biol.* 5. <https://doi.org/10.1038/s42003-022-03466-x>.
- Makropoulos, A., et al., 2018. The developing human connectome project: a minimal processing pipeline for neonatal cortical surface reconstruction. *Neuroimage* 173, 88–112. <https://doi.org/10.1016/j.neuroimage.2018.01.054>.
- Martino, J., Brogna, C., Robles, S.G., Vergani, F., Duffau, H., 2010. Anatomic dissection of the inferior fronto-occipital fasciculus revisited in the lights of brain stimulation data. *Cortex* 46, 691–699. <https://doi.org/10.1016/j.cortex.2009.07.015>.
- Miller, D.J., Dukka, T., Stimpson, C.D., Schapiro, S.J., Baze, W.B., McArthur, M.J., Hobbs, A.J., Sousa, A.M.M., Sestan, N., Wildman, D.E., Lipovich, L., Kuzawa, C.W., Hof, P.R., Sherwood, C.C., 2012. Prolonged myelination in human neocortical evolution. *P. Natl. Acad. Sci. USA* 109, 16480–16485. <https://doi.org/10.1073/pnas.1117943109>.
- Mongerson, C.R., Jennings, R.W., Borsook, D., Becerra, L., Bajic, D., 2017. Resting-state functional connectivity in the infant brain: methods, pitfalls, and potentiality. *Front. Pediatr.* 5, 159. <https://doi.org/10.3389/fped.2017.00159>.
- Nair, A., Jalal, R., Liu, J., Tsang, T., McDonald, N.M., Jackson, L., Ponting, C., Jeste, S.S., Bookheimer, S.Y., Dapretto, M., 2021. Altered thalamocortical connectivity in 6-week-old infants at high familial risk for autism spectrum disorder. *Cereb. Cortex* 31, 4191–4205. <https://doi.org/10.1093/cercor/bhab078>.
- Ouyang, M.H., Dubois, J., Yu, Q.L., Mukherjee, P., Huang, H., 2019. Delineation of early brain development from fetuses to infants with diffusion MRI and beyond. *Neuroimage* 185, 836–850. <https://doi.org/10.1016/j.neuroimage.2018.04.017>.
- Prete, M.G., Van De Ville, D., 2019. Decoupling of brain function from structure reveals regional behavioral specialization in humans. *Nat. Commun.* 10, 4747. <https://doi.org/10.1038/s41467-019-12765-7>.
- Qiu, A., Mori, S., Miller, M.I., 2015. Diffusion tensor imaging for understanding brain development in early life. *Annu. Rev. Psychol.* 66, 853–876. <https://doi.org/10.1146/annurev-psych-010814-015340>.
- Rees, P., Callan, C., Chadda, K.R., Vaal, M., Diviney, J., Sabti, S., Harnden, F., Gardiner, J., Battersby, C., Gale, C., Sutcliffe, A., 2022. Preterm brain injury and neurodevelopmental outcomes: a meta-analysis. *Pediatrics* 150. <https://doi.org/10.1542/peds.2022-057442>.
- Rogers, C.E., Lean, R.E., Wheelock, M.D., Smyser, C.D., 2018. Aberrant structural and functional connectivity and neurodevelopmental impairment in preterm children. *J. Neurodev. Disord.* 10, 38. <https://doi.org/10.1186/s11689-018-9253-x>.
- Roze, E., Reijneveld, S.A., Stewart, R.E., Bos, A.F., 2021. Multi-domain cognitive impairments at school age in very preterm-born children compared to term-born peers. *BMC Pediatr.* 21, 169. <https://doi.org/10.1186/s12887-021-02641-z>.
- Saigal, S., Doyle, L.W., 2008. An overview of mortality and sequelae of preterm birth from infancy to adulthood. *Lancet* 371, 261–269. [https://doi.org/10.1016/S0140-6736\(08\)60136-1](https://doi.org/10.1016/S0140-6736(08)60136-1).
- Seguin, C., Sporns, O., Zalesky, A., 2023. Brain network communication: concepts, models and applications. *Nat. Rev. Neurosci.* 24, 557–574. <https://doi.org/10.1038/s41583-023-00718-5>.
- Shi, F., Yap, P.-T., Wu, G., Jia, H., Gilmore, J.H., Lin, W., Shen, D., 2011. Infant brain atlases from neonates to 1-and 2-year-olds. *PLoS One* 6, e18746. <https://doi.org/10.1371/journal.pone.0018746>.
- Shi, F., Yap, P.-T., Gao, W., Lin, W., Gilmore, J.H., Shen, D., 2012. Altered structural connectivity in neonates at genetic risk for schizophrenia: a combined study using morphological and white matter networks. *Neuroimage* 62, 1622–1633.
- Shi, Y., Budin, F., Yapuncich, E., Rumple, A., Young, J.T., Payne, C., Zhang, X., Hu, X., Godfrey, J., Howell, B., 2017. UNC-Emory infant atlases for macaque brain image analysis: postnatal brain development through 12 months. *Front. Neurosci.* 10, 617. <https://doi.org/10.3389/fnins.2016.00617>.
- Sie, L.T., Van Der Knaap, M.S., Van Wezel-Meijler, G., Valk, J., 1997. MRI assessment of myelination of motor and sensory pathways in the brain of preterm and term-born infants. *Neuropediatrics* 28, 97–105. <https://doi.org/10.1055/s-2007-973680>.
- Smith, S.M., Beckmann, C.F., Andersson, J., Auerbach, E.J., Bijsterbosch, J., Douaud, G., Duff, E., Feinberg, D.A., Griffanti, L., Harms, M.P., 2013. Resting-state fMRI in the human connectome project. *Neuroimage* 80, 144–168. <https://doi.org/10.1016/j.neuroimage.2013.05.039>.
- Soman, S.M., Vijayakumar, N., Thomson, P., Ball, G., Hyde, C.S., Silk, T.J., 2023. Cortical structural and functional coupling during development and implications for attention deficit hyperactivity disorder. *ARTN 252 Transl. Psychiatr* 13. <https://doi.org/10.1038/s41398-023-02546-8>.
- Suarez, L.E., Markello, R.D., Betzel, R.F., Misic, B., 2020. Linking structure and function in macroscale brain networks. *Trends Cogn. Sci.* 24, 302–315. <https://doi.org/10.1016/j.tics.2020.01.008>.
- Suárez, L.E., Markello, R.D., Betzel, R.F., Misic, B., 2020. Linking structure and function in macroscale brain networks. *Trends Cogn. Sci.* 24, 302–315. <https://doi.org/10.1016/j.tics.2020.01.008>.
- Sun, H., Jiang, R., Dai, W., Dufford, A.J., Noble, S., Spann, M.N., Gu, S., Scheinost, D., 2023. Network controllability of structural connectomes in the neonatal brain. *Nat. Commun.* 14, 5820. <https://doi.org/10.1038/s41467-023-41499-w>.
- Thomason, M.E., Scheinost, D., Manning, J.H., Grove, L.E., Hect, J., Marshall, N., Hernandez-Andrade, E., Berman, S., Pappas, A., Yeo, L., Hassan, S.S., Constable, R.T., Ment, L.R., Romero, R., 2017. Weak functional connectivity in the human fetal brain prior to preterm birth. *ARTN 39286 Sci. Rep.* -Uk 7. <https://doi.org/10.1038/srep39286>.
- Thompson, D.K., Chen, J., Beare, R., Adamson, C.L., Ellis, R., Ahmadzai, Z.M., Kelly, C.E., Lee, K.J., Zalesky, A., Yang, J.Y.M., Hunt, R.W., Cheong, J.L.Y., Inder, T.E., Doyle, L.W., Seal, M.L., Anderson, P.J., 2016. Structural connectivity relates to perinatal factors and functional impairment at 7years in children born very preterm. *Neuroimage* 134, 328–337. <https://doi.org/10.1016/j.neuroimage.2016.03.070>.
- Vandewouw, M.M., Hunt, B.A.E., Ziolkowski, J., Taylor, M.J., 2021. The developing relations between networks of cortical myelin and neurophysiological connectivity. *Neuroimage* 237, 118142. <https://doi.org/10.1016/j.neuroimage.2021.118142>.
- Vázquez-Rodríguez, B., Suárez, L.E., Markello, R.D., Shahiei, G., Paquola, C., Hagmann, P., Van Den Heuvel, M.P., Bernhardt, B.C., Spreng, R.N., Misic, B., 2019. Gradients of structure-function tethering across neocortex. *Proc. Natl. Acad. Sci.* 116, 21219–21227. <https://doi.org/10.1073/pnas.1903403116>.
- Yeo, B.T., Krienen, F.M., Sepulcre, J., Sabuncu, M.R., Lashkari, D., Hollinshead, M., Roffman, J.L., Smoller, J.W., Zöllei, L., Polimeni, J.R., 2011. The organization of the human cerebral cortex estimated by intrinsic functional connectivity. *J. Neurophysiol.* <https://doi.org/10.1152/jn.00338.2011>.
- Yeo, B.T.T., Krienen, F.M., Eickhoff, S.B., Yaakub, S.N., Fox, P.T., Buckner, R.L., Asplund, C.L., Chee, M.W.L., 2014. Functional specialization and flexibility in human association cortex. *Cereb. Cortex* 25, 3654–3672. <https://doi.org/10.1093/cercor/bhu217>.
- Yu, Q., Ouyang, M., Detre, J., Kang, H., Hu, D., Hong, B., Fang, F., Peng, Y., Huang, H., 2023. Infant brain regional cerebral blood flow increases supporting emergence of the default-mode network. *eLife* 12, e78397. <https://doi.org/10.7554/eLife.78397>.
- Zarkali, A., McColligan, P., Leyland, L.-A., Lees, A.J., Rees, G., Weil, R.S., 2021. Organisational and neuromodulatory underpinnings of structural-functional connectivity decoupling in patients with Parkinson's disease. *Commun. Biol.* 4, 86. <https://doi.org/10.1038/s42003-020-01622-9>.
- Zhang, S., He, Z.B., Du, L., Zhang, Y., Yu, S.G., Wang, R.Y., Hu, X.T., Jiang, X., Zhang, T., 2021. Joint analysis of functional and structural connectomes between preterm and term infant brains via canonical correlation analysis with locality preserving projection. *ARTN 724391 Front. Neurosci.* 15. <https://doi.org/10.3389/fnins.2021.724391>.
- Zheng, W.H., Wang, X.M., Liu, T.T., Hu, B., Wu, D., 2023. Preterm-birth alters the development of nodal clustering and neural connection pattern in brain structural network at term-equivalent age. *Hum. Brain Mapp.* 44, 5372–5386. <https://doi.org/10.1002/hbm.26442>.